

DYNAMICS OF LINE-DRIVEN WINDS FROM DISKS IN CATAclySMIC VARIABLES. II. MASS-LOSS RATES AND VELOCITY LAWS

ACHIM FELDMEIER AND ISAAC SHLOSMAN

Department of Physics and Astronomy, University of Kentucky, Lexington, KY 40506-0055; achim@pa.uky.edu, shlosman@pa.uky.edu

AND

PETER VITELLO

Lawrence Livermore National Laboratory, L-282, P.O. Box 808, Livermore, CA 94550; vitello@llnl.gov

Received 1999 February 9; accepted 1999 July 2

ABSTRACT

We analyze the dynamics of two-dimensional stationary, line-driven winds from accretion disks in cataclysmic variable (CV) stars by generalizing the formalism of Castor, Abbott, and Klein (CAK) for O stars. In Paper I, we solved the wind Euler equation, derived its two eigenvalues, and addressed the solution topology and wind geometry. Here, we focus on mass-loss rates and velocity laws of the wind. We find that disk winds, even in luminous nova-like variables, have low optical depth, even in the strongest driving lines. This suggests that thick-to-thin transitions in these lines occur in the wind. For disks with a realistic radial temperature law, the mass loss is dominated by gas emanating from the inner decade in radius. The total mass-loss rate associated with the wind from a disk of luminosity $10 L_{\odot}$ is $\sim 10^{-12} M_{\odot} \text{ yr}^{-1}$, or 10^{-4} of the mass accretion rate. This is 1 order of magnitude below the lower limit obtained from fitting P Cygni line profiles using kinematical wind models when the Lyman continuum is suppressed. The difficulties associated with such small mass-loss rates for line-driven winds from disks in CVs are principal and confirm our previous work on this subject. We conjecture that this issue may be resolved by detailed non-LTE calculations of the CAK line force within the context of CV disk winds and/or by better accounting for the disk energy distribution and wind ionization structure. We find that the wind velocity profile is well approximated by the empirical law used in kinematical modeling. The acceleration length scale is given by the footpoint radius of the wind streamline in the disk. This suggests an upper limit of $\sim 10 r_{\text{wd}}$ to the acceleration scale, which is smaller by factor of a few as compared with values derived from line fitting.

Subject headings: accretion, accretion disks — novae, cataclysmic variables — stars: mass loss — stars: winds, outflows

1. INTRODUCTION

Line-driven winds (hereafter LDWs) are expected around luminous objects the spectra of which peak in the UV, such as OB stars and accretion disks, stellar and galactic (Vitello & Shlosman 1988). Feldmeier & Shlosman (1999, hereafter Paper I) have investigated a two-dimensional analytical model of LDWs from disks in cataclysmic variables (CVs) characterized by a large mass transfer rate from the secondary to the white dwarf. Such CVs, i.e., nova-like variables and dwarf novae in outburst, show clear signs of outflows driven by radiation pressure (Paper I and references therein).

Recent numerical simulations of time-dependent two-dimensional disk winds by Proga, Stone, & Drew (1998; hereafter PSD) largely confirmed the previous kinematical studies by Shlosman & Vitello (1993) and Knigge, Woods, & Drew (1995) and delineated a number of empirical relationships that require further physical explanation. Paper I has addressed the two-dimensional geometry of the wind streamlines and the topology of solutions to the wind momentum equation. In particular, a comparison with the PSD model was made as well as a comparison with the one-dimensional LDWs from OB stars.

The main results of Paper I are as follows. First, the solutions to the wind momentum equation are characterized by two eigenvalues, the mass-loss rate and the flow tilt angle with the disk, in the presence of a realistic radiation field above the disk. The existence of the second eigenvalue is a reflection of the multidimensional nature of a disk wind.

The wind itself appears to be collimated to a certain degree, i.e., the wind collimation angle with the rotation axis (semi-opening angle) is about 10° for the wind launched within four white dwarf radii, and about 30° for the outer wind, for the Shakura & Sunyaev (1973, hereafter SHS) disk. Furthermore, the wind collimation solely depends on the radial temperature stratification in the disk, unless there is an additional degree of freedom such as a central luminosity associated with nuclear burning on the surface of the white dwarf or with a boundary layer. The above degree of collimation for disk winds in CVs should be taken with caution at large distances from the disk.

Second, a major distinction between stellar and disk LDWs is the existence of maxima in both the gravity and the radiation flux above the disk. This behavior of gravity and radiation flux results in profound topological differences in the solutions to the stellar and disk wind momentum equations. We find that two distinct regions of disk wind exist, the inner and outer winds. The critical point of the outer wind lies close to the disk photosphere and to the sonic point, upstream of the top of the gravity “hill.” This proximity of the critical and sonic points is typical of LDWs from O stars as well. On the other hand, for the inner wind, the critical point lies far away from the sonic point, beyond the gravity hill.

Observationally, the mass-loss rates from CV disk winds are poorly constrained. This is mainly a consequence of uncertainties in the ionizing fluxes from different com-

ponents in the system and, therefore, of the ionization stratification of the wind. Neglecting the boundary layer and assuming a local blackbody radiation from the disk, Vitello & Shlosman (1993) and Knigge et al. (1995) find wind mass-loss rates $\sim 1\%$ of the accretion rate by fitting observed P Cygni line profiles. For a system with luminosity $10 L_{\odot}$, this corresponds to a mass-loss rate of about $2 \times 10^{-10} M_{\odot} \text{ yr}^{-1}$.

These mass-loss rates are *upper* limits for the following reason. The radiation field in the Lyman continuum is often found to be highly suppressed compared to blackbody emission or stellar photospheric fluxes, or it may even be absent (Polidan, Mauche, & Wade 1990; Long et al. 1991, 1994; van Teeseling, Verbunt, & Heise 1993; Knigge et al. 1997). This drastic reduction in ionizing flux allows a reduction in the electron density and, therefore, in the mass-loss rate from the disk, \dot{M} , while maintaining the same degree of ionization in the wind.

On the other hand, a reasonable *lower* limit to the wind mass-loss rate from luminous CV disks was found by Prinja & Rosen (1995). They argued that the product $\dot{M}q$, where q is the ionization fraction of C IV, lies between 5×10^{-13} and $1 \times 10^{-11} M_{\odot} \text{ yr}^{-1}$ for 10 dwarf novae and nova-like variables with high-resolution *IUE* spectra (see also Mauche & Raymond 1987; Hoare & Drew 1993). This results in a lower limit of $\dot{M} \sim 5 \times 10^{-13} M_{\odot} \text{ yr}^{-1}$. Note that this value is still model dependent to some degree, since Prinja & Rosen assumed a constant ionization fraction throughout the wind and a purely radial flow.

In this paper, we focus on the mass-loss rate and the velocity law of disk LDWs in CVs. We employ the main assumption of Paper I that the wind streamlines are contained in straight cones, the collimation angles of which are eigenvalues of the Euler equation. This approximation is acceptably close to the disk (e.g., as shown by PSD) and allows us to make a meaningful determination of the mass-loss rate (which is constrained close to the disk photosphere as well) and of the initial velocity law. A similar conclusion was reached from line fitting using two-dimensional wind kinematics (Vitello & Shlosman 1993; Knigge et al. 1995). On the other hand, we expect both the centrifugal forces and the polar component of the line force to bend the streamlines at large distances from the disk and to influence the terminal velocity of the flow.

This paper is organized as follows. Section 2 reviews the mass-loss rates derived from the theory of Castor, Abbott, & Klein (1975, hereafter CAK). Section 3 shows that CV disk winds are expected to have low optical depth even in strong lines. Sections 4 and 5 derive the mass-loss rates and velocity laws for the disk wind model. Sections 6 and 7 discuss and summarize our results.

2. CAK MASS-LOSS RATES FOR STARS AND CV DISKS

The CAK line force for stellar winds is fully determined by two parameters, the power exponent α and the mass absorption coefficient of the strongest driving line, κ_0 (Paper I; Puls, Springmann, & Lennon 1999). Instead of using κ_0 directly, CAK parameterize the line force per unit mass as $g_L = M(t)g_e$, where $M(t) \equiv kt^{-\alpha}$ (with $0 < \alpha < 1$) is the so-called force multiplier, and g_e is the force caused by electron scattering. The optical depth t refers to a line with $\kappa = \sigma_e$, where σ_e is the electron scattering coefficient. The

parameter k is given in terms of κ_0 by

$$k = \frac{\Gamma(\alpha)}{1 - \alpha} \frac{v_{\text{th}}}{c} \left(\frac{\kappa_0}{\sigma_e} \right)^{1-\alpha}, \quad (1)$$

where $\Gamma(\alpha)$ is the complete gamma function, c is the speed of light, and v_{th} is the thermal speed of carbon ions (CAK) or hydrogen (Abbott 1982). The above parameterization for $M(t)$ as a power law, however, does not account correctly for optically thin winds, where the force multiplier saturates at some value $M_{\text{max}}(t) \equiv Q \sim 2000$ for a gas of solar composition (Abbott 1982). Gayley (1995) noted that Q is essentially identical to the Q -value of a resonator and can be estimated as $Q \sim A \nu/\gamma$, where $A \sim 10^{-4}$ is the abundance of valence electrons, $\nu \sim 10^{15} \text{ s}^{-1}$ is the frequency of UV radiation, and $\gamma \sim 10^8 \text{ s}^{-1}$ is the damping rate. Hence, $Q \sim 1000$ should be an appropriate value for O stars. However, for winds from B stars near the main sequence, modeling of X-ray spectra already suggests that appropriate Q -values differ from those for O stars. The mass-loss rates inferred from the standard theory can be substantially lower than the inferred ones (Cassinelli 1994; Cassinelli et al. 1994).

In terms of Q , κ_0 is given by (Gayley 1995)

$$\frac{\kappa_0 v_{\text{th}}}{\sigma_e c} = \Gamma(\alpha)^{-[1/(1-\alpha)]} Q. \quad (2)$$

Inserting the eigenvalue E_{cr} from equation (8b) in Paper I into equation (6) thereof, the CAK mass-loss rate from O-star winds takes the compact form,

$$\dot{M} = \frac{\alpha}{1 - \alpha} \left(\frac{Q \Gamma}{1 - \Gamma} \right)^{(1-\alpha)/\alpha} \frac{L}{c^2}, \quad (3)$$

with luminosity L and the Eddington factor Γ . This expression is valid as long as $Q \Gamma/(1 - \Gamma) > 1$. Otherwise, the gravity prevails and no wind solution exists. For the above value of Q , and assuming $\alpha = \frac{2}{3}$ and an Eddington factor $\Gamma = 0.5$ of an O supergiant, equation (3) gives $\dot{M} \sim 90L/c^2$. Thus, the mass-loss rate from the CAK theory agrees well with the estimate from the single scattering limit, $\dot{M} = (c/v_{\infty})(L/c^2) \sim 100L/c^2$, for typical wind terminal speeds $v_{\infty} \sim 3000 \text{ km s}^{-1}$. However, agreement between both mass-loss rates is solely the result of Γ being close to unity.

If, alternatively, $\Gamma \ll 1$, the CAK mass-loss rate falls well below the single scattering limit. As we show in § 3, the mass loss of a disk LDW is given again by equation (3), up to correction factors of order unity. Even for the brightest CVs, i.e., nova-like variables and dwarf novae in eruption, which experience LDWs, $Q\Gamma \sim 1$ (applying the O-star value of Q). Hence, $\dot{M} \sim L/c^2$ from equation (3), whereas the single scattering limit gives $\dot{M} \sim 60 L/c^2$, for $v_{\infty} \sim 5000 \text{ km s}^{-1}$. Since in thin LDWs the probability for a photon to be scattered by a line is less than unity, the estimate from the single scattering is way too high (see also Puls, Springmann, & Owocki 1998).

3. DISK WIND OPTICAL DEPTHS

A number of fundamental differences exist between stellar and disk LDWs in CVs, some of which have been discussed in Paper I. Here we show that optical depths for CV winds are more typical of thin winds, e.g., of B stars near the main sequence, than of more extensive supergiant winds.

3.1. Disk Wind Geometry and Radiation Field

The disk wind geometry is described in Paper I, and we repeat here only the essential assumptions and make necessary definitions. A flow streamline is a helix that is contained within a *straight cone* (Fig. 1). The footpoint radius of a streamline in the disk is r_0 , the tilt of the cone with the disk is λ , and x is the distance along the cone. We neglect pressure forces and assume that the azimuthal velocity is determined by angular momentum conservation above the disk and by Keplerian rotation within the disk. The only remaining velocity component is v_x , which points upward along the cone. We introduce a normalized coordinate $X \equiv x/r_0$. The velocity V is normalized to the local escape speed, and the flow acceleration becomes $W' = dW/dX = 2V dV/dX$. Last, we introduce the radiation flux F above the disk and the flux \tilde{F} normalized to the footpoint flux of the streamline, as well as their projected counterparts F_x and \tilde{F}_x along the wind cone (§ 3.2 of Paper I).

3.2. Semitransparent Winds from CV Disks?

In this section, we make use of a simplified Euler equation for the disk LDW to show explicitly that low Γ factors in CV disks imply low optical depths in the wind. By doing so, we neglect factors of order unity from the angle integration in equation (2) of Paper I, in replacing the optical depth, τ_y , in arbitrary direction \hat{y} by the optical depth in flow direction, $\tau_y = \tau_x$. For the sake of simplicity, only the disk with $F \propto r_0^{-2}$ (hereafter termed “Newtonian” disk) is considered. The line force per unit mass is then

$$g_L = \frac{\sigma_e F_x(r_0, X)}{c} M(t_x) = \frac{\sigma_e F_z(r_0, 0)}{c} \tilde{F}_x(r_0, X) M(t_x). \quad (4)$$

The Euler equation for the disk wind, in the limit of zero sound speed, and neglecting the force caused by electron scattering because of small Γ above the disk, becomes (with gravitational constant G , white dwarf mass M_{wd} , dimensional wind speed v_x , and $v'_x = dv_x/dx$),

$$v_x v'_x = -\frac{GM_{\text{wd}}}{r_0^2} [g(X) - \Gamma(r_0) \tilde{F}_x(r_0, X) M(t_x)], \quad (5)$$

where the effective gravity g was defined in equation (9) of Paper I, and we introduced

$$\Gamma(r_0) \equiv \frac{\sigma_e F_z(r_0, 0) r_0^2}{cGM_{\text{wd}}}. \quad (6)$$

For the Newtonian disk, $\Gamma(r_0) = \sigma_e L_d / [4\pi cGM_{\text{wd}} \ln(r_d/r_{\text{wd}})]$ becomes *independent* of r_0 . Here, L_d is the disk luminosity, and r_d and r_{wd} are the outer and inner disk radii,

– 26 –

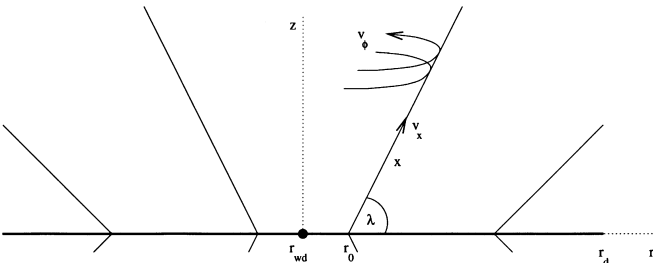


FIG. 1.—Adopted flow geometry for a CV disk wind. The streamlines are helical lines and are assumed to lie on straight cones.

with r_{wd} being the white dwarf radius. Using typical parameters for nova-like CVs, $L_d = 10 L_\odot$, $M_{\text{wd}} = 0.7 M_\odot$, and $r_d/r_{\text{wd}} = 30$, one has that $\Gamma \simeq 10^{-4}$.

For a stationary wind solution to exist, the right-hand side of equation (5) has to be positive. This poses a constraint on $M(t)$ and therefore on t . Namely, the maximum of reduced gravity g lies between $2/(3 \times 3^{1/2}) \simeq 0.38$ for $\lambda = 90^\circ$ and $4/27 \simeq 0.15$ for $\lambda = 0^\circ$. Since \tilde{F}_x is of order unity (see Fig. 5 in Paper I), $M(t)$ approaches its maximum value, Q , in regions of large gravity and stays constant thereafter. In other words, because Γ is so small for CV disks, the wind solution barely “makes it” over the gravity hill.

This saturation effect in $M(t)$ happens when the strongest driving line in the wind becomes optically thin, at about $t \sim 10^{-7}$. If this thick-to-thin transition occurs before or at the critical point of the flow, the wind solution is lost. This possibility cannot be excluded in our model given the rapid change of the velocity gradient (and hence of t) in the vicinity of the critical point. The consequences of this effect on the feasibility of LDWs are discussed in § 6.

The situation is fundamentally different for dense winds of O stars, where the Euler equation for the radial wind speed, v_r , reads (with M being the stellar mass)

$$v_r v'_r = -\frac{GM}{r^2} \left(1 - \Gamma[M(t) + 1] \right). \quad (7)$$

Assuming $\Gamma > 0.1$ for O stars, there is a wide range in $M(t)$ for a stationary solution to exist, namely ~ 10 –2000. The highest mass-loss rate solution (hence, the slowest wind) is characterized by the lowest allowable $M(t) \sim 10$. The permitted range in $M(t)$ corresponds to an even wider range in t (because $\alpha < 1$), $t \sim 10^{-7}$ to 10^{-3} . We further quantify these arguments in the Appendix.

Our estimate for t in CV winds contradicts the claim by Murray & Chiang (1996) that the optical depth parameter t is similar for CV disk and O-star winds.

4. DISK WIND MASS-LOSS RATES

4.1. Vertical Disk Wind

The mass-loss rate of the vertical wind above an isothermal disk is determined by the eigenvalue E_{cr} in equation (18b) in Paper I. From equation (17) in Paper I, one finds

$$\dot{M} = \frac{\alpha}{1 - \alpha} \left(\frac{3\sqrt{3}c\sigma_e Q}{8\pi GM_{\text{wd}}} \right)^{(1-\alpha)/\alpha} D \left(\frac{L_d}{c^2} \right)^{1/\alpha}. \quad (8)$$

The dimensionless constant D is given by

$$D = \int_{r_1}^{r_2} \frac{dr_0}{r_0} \left[\frac{4\pi r_0^2 F_z(r_0, 0)}{L_d} \right]^{1/\alpha}, \quad (9)$$

where r_1 and r_2 are the inner and outer radii of the wind base in the disk, respectively. Making the plausible assumptions that $r_d \gg r_{\text{wd}}$, $r_2 \gg r_1$, and $r_2 \simeq r_d$ (both of the latter radii are determined essentially by the temperature dropping below 10^4 K), we estimate $D \simeq 1$ for $\alpha = \frac{1}{2}$ and $\alpha = \frac{2}{3}$. Introducing a new, global disk Eddington factor,

$$\Gamma_d = \frac{\sigma_e L_d}{4\pi cGM_{\text{wd}}}, \quad (10)$$

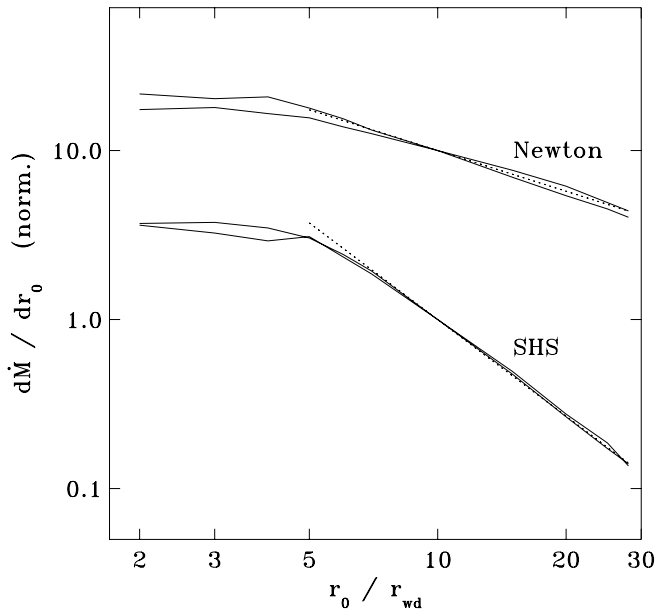


FIG. 2.—Mass-loss rate per disk annulus, $d\dot{M}/dr_0$, as function of foot-point radius, r_0 . Table 1 and eq. (17) from Paper I were used for SHS and Newtonian disks with $\alpha = \frac{2}{3}$ and $\alpha = \frac{1}{2}$. Dotted lines are fits with $d\dot{M}/dr_0 \propto r_0^{-1.9}$ (SHS) and $\propto r_0^{-0.8}$ (Newtonian). The curves are normalized at $r_0/r_{wd} = 10$.

equation (8) becomes

$$\dot{M} \simeq \frac{\alpha}{1-\alpha} \left(\frac{3\sqrt{3}}{2} Q \Gamma_d \right)^{(1-\alpha)/\alpha} \frac{L_d}{c^2}. \quad (11)$$

Up to the correction factors caused by different gravity (and geometry), this equation is identical to the CAK mass-loss rate from a point star, equation (3). Note that a disk wind is more efficient in carrying mass loss than an O-star wind by a factor of $[(3 \times 3^{1/2})/2]^{(1-\alpha)/\alpha}$, owing to the lower gravity potential well. Rewriting equation (11) as $\dot{M} \equiv N L_d / c^2$ (where the coefficient N depends on L_d), and using the relevant parameters for nova-like CVs introduced above, gives $N \simeq 2$ and a disk mass-loss rate $\dot{M} \simeq 10^{-12} M_\odot \text{ yr}^{-1}$ for $Q = 2000$.

4.2. Tilted Disk Winds

A more realistic picture of disk mass loss consists of a tilted wind from a disk with radial temperature stratification. From equation (17) in Paper I, using equation (10),

$$\dot{M} = \frac{\alpha}{1-\alpha} \left(\frac{3\sqrt{3}}{2} Q \Gamma_d \right)^{(1-\alpha)/\alpha} D \langle \dot{m} \rangle \frac{L_d}{c^2}, \quad (12)$$

where

$$\langle \dot{m} \rangle \equiv \int_{r_1}^{r_2} \frac{dr_0}{r_0} \dot{m}(r_0) [r_0^2 F_z(r_0, 0)]^{1/\alpha} / \int_{r_1}^{r_2} \frac{dr_0}{r_0} [r_0^2 F_z(r_0, 0)]^{1/\alpha}, \quad (13)$$

and $\dot{m}(r_0)$ is normalized in units of mass loss from a vertical wind; $\langle \dot{m} \rangle$ is then a normalized mass-loss rate per dr_0 , averaged over the wind base. Using values of $\dot{m}(r_0)$ from Table 1 in Paper I, we estimate $\langle \dot{m} \rangle = 1.2$ for $\alpha = \frac{2}{3}$, and $\langle \dot{m} \rangle = 2.2$ for $\alpha = \frac{1}{2}$, both for SHS and Newtonian disks. For the latter, one has $D = \ln(r_2/r_1) / [\ln(r_d/r_{wd})]^{1/\alpha}$. This expression is roughly correct also for the SHS disk, where D cannot be calculated analytically. Inserting the values for

$\langle \dot{m} \rangle$ and D into equation (12), one finds, for $\alpha = \frac{1}{2}$ and $\alpha = \frac{2}{3}$, and for SHS and the Newtonian disks, assuming once again typical parameters for nova-like CVs and $Q = 2000$, that $N \simeq 2$ or $\dot{M} \simeq 10^{-12} M_\odot \text{ yr}^{-1}$.

Interestingly, the mass-loss rates for a vertical wind above an isothermal disk and for tilted winds above disks with temperature stratification are very similar. This means that the disk mass-loss rate is only a weak function of the tilt angle, as long as the latter is aligned with the radiation flux. For the disk types used in the present work, this range encompasses $\lambda \sim 50^\circ - 90^\circ$, according to Table 1 in Paper I.

It is readily shown that the mass-loss rate for an LDW due to a single, optically thick line is roughly L_d/c^2 . The above $N \simeq 2$, therefore, implies that only a few lines become optically thick in the present CV disk wind model. Unlike for disk winds, in O-star winds of the order of 100 lines become optically thick, according to equation (3).

Note that in Paper I, eigenvalues E were derived *without* including the saturation of the force multiplier at $M_{\max}(t) = Q$ (i.e., without applying the exponential line-list cutoff of Owocki, Castor, & Rybicki 1988). The above mass-loss rates are, therefore, upper limits.

Finally, we derive the dependence of the mass-loss rate $d\dot{M}$ on r_0 . According to equation (17) in Paper I, this relation is determined by the disk temperature stratification and the run of E_{cr} with r_0 . For an isothermal disk, E_{cr} was found to be independent of r_0 , hence $d\dot{M}/dr_0 \propto r_0^{(2-\alpha)/\alpha}$. Such an unrealistic growth of $d\dot{M}/dr_0$ with radius is a consequence of the increase of radiation energy with r_0 . For the Newtonian disk, Figure 2 shows $d\dot{M}/dr_0$ according to Table 1 and equation (17) in Paper I. A good power-law fit to the eigenvalues is given by $d\dot{M}/dr_0 \propto r_0^{-0.8}$ for $r_0 \gtrsim 5r_{wd}$. The total disk mass-loss rate therefore scales roughly as $\dot{M} \propto \ln r_2$. For the SHS disk, Figure 2 gives approximately $d\dot{M}/dr_0 \propto r_0^{-1.9}$ for $r_0 \gtrsim 5r_{wd}$; hence, the total \dot{M} should depend on r_2 only very weakly. At $r_0 \lesssim 5r_{wd}$, the radial dependency of $d\dot{M}/dr_0$ is weak for both types of disks. Therefore, the mass-loss rate \dot{M} is centrally concentrated—and more so for SHS disks.

5. VELOCITY LAWS FOR DISK WINDS

We discuss the wind velocity law by solving the Euler equation, first neglecting, then accounting for ionization effects in the flow. Only the flow above the SHS disk is analyzed in this section.

5.1. Solutions to the Algebraic Euler Equation

The geometrical expansion terms, discussed in § 5.1 of Paper I, introduce a velocity dependency into the wind Euler equation. However, we find that these terms leave the mass-loss rates in the model practically unchanged and increase the wind velocity by at most 10%. The reason for this is the small angle dispersion in the wind streamlines. Therefore, we omit geometrical expansion terms here.

Without explicit dependence on velocity, the Euler equation becomes purely algebraic. Figure 8 of Paper I displays the solutions $W'(X)$ of the Euler equation (20) thereof for a tilted disk wind at different r_0 . The velocity field above the disk is obtained by integrating W' and is displayed for a number of streamlines in Figure 3 for the SHS disk and $\alpha = \frac{2}{3}$. As shown in Paper I, the LDW velocity law is not necessarily a monotonic function of X . Clearly, the deceleration regime (marked with a cross in Fig. 3) is unimportant for streamlines starting at large r_0 , because it lies at large X

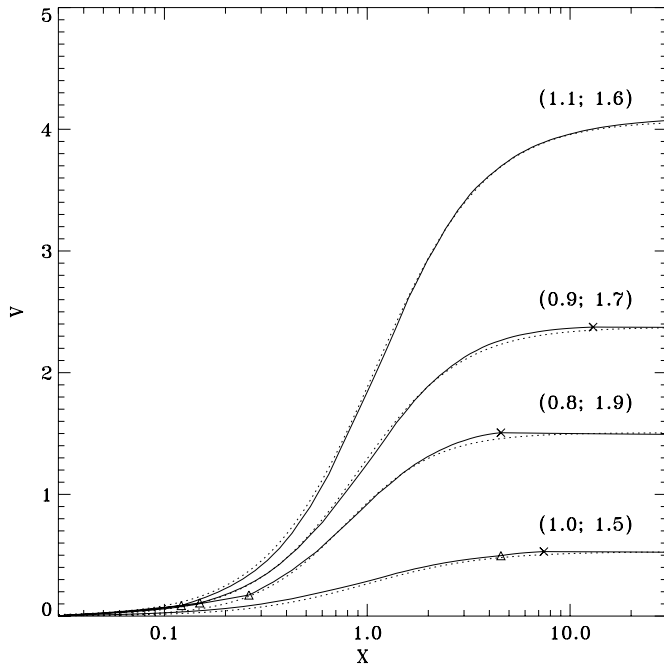


FIG. 3.—Velocity profiles for the SHS disk with $r_d = 30r_{wd}$, for $\alpha = \frac{2}{3}$, and at footpoint radii 3, 7, 10, $15r_{wd}$ (from bottom to top). The dotted lines are fits using the velocity law eq. (14), with the values of $(X_{acc}; \beta)$ given in brackets. The velocity V is in units of the local escape speed at r_0 . For the tilt angles, eigenvalues λ_{cr} from Paper I were used. Triangles mark the critical point, and crosses mark the point where the wind starts to decelerate.

where the flow moves much faster than the local escape speed. The inner streamlines do show a more pronounced kink.

The wind terminal velocities are found to be independent of r_0 , for $\alpha = \frac{1}{2}$, and linearly dependent on r_0 for $\alpha = \frac{2}{3}$, growing by a factor of 5 over the whole disk. However, this may be of academic interest only, since the wind is expected to go through an optically thick-to-thin transition beforehand. Hence the actual observable terminal velocities may be smaller.

The velocity profiles in Figure 3 are well approximated by the empirical velocity law used by Shlosman & Vitello (1993) in fitting the line profiles of nova-like CVs,

$$v = v_\infty \frac{(X/X_{acc})^\beta}{1 + (X/X_{acc})^\beta}. \quad (14)$$

Here, X_{acc} is the acceleration length scale along the wind cone. We find the best fits to Figure 3 for $\beta = 1.5$ – 1.9 . Vitello & Shlosman quote rather similar values of $\beta = 1.3$ – 1.5 . Furthermore, $X_{acc} \approx 1$ in Figure 3, which means that the footpoint radius r_0 sets the acceleration length. The reason for this is that X_{acc} is determined by the effective gravity and disk radiation field, i.e., by the auxiliary functions g and f (Paper I), which change on length scales $\sim r_0$. For this reason, we do not expect X_{acc} to depend on α . The X_{acc} from observed P Cygni line profiles are usually found to be larger, namely, in the range 1–10 (Hoare & Drew 1993; Vitello & Shlosman 1993), depending on individual objects. We comment further on this in § 6.3.

5.2. Effects of Ionization Stratification in the Wind

The major concern of the present model is the small optical depth in the wind, making the latter semitransparent

even in the strongest driving lines, when $Q = 2000$ is used. The resolution of this problem may be related to the ionization structure in the wind, which is expected to lead to a more shallow velocity law and smaller velocity gradients. We parameterize the ionization stratification in the simplest possible way by introducing the $\delta (> 0)$ parameter customarily used in stellar wind theory (e.g., Abbott 1982), namely,

$$g_L \propto t^{-\alpha} \xi^{-\delta}, \quad (15)$$

where $\xi \equiv J/n_e$ is the ionization parameter, J is the frequency-integrated mean intensity, and n_e is the electron number density. Higher ionization stages typically harbor fewer lines than lower ionization stages and therefore lead to a smaller line force. Typical values for O stars are $\delta \lesssim 0.1$ (Abbott 1982; Puls 1987; Pauldrach et al. 1994), but values as large as $\delta = 0.7$ have been suggested recently for winds at low effective temperatures of 8000 K (Kudritzki et al. 1998).

To include the δ -correction term in the present model, we calculate first dJ from a disk annulus of radius q and width dq , using cylindrical coordinates r and z ,

$$dJ(r, z) = 4I(q, 0)q dqz \frac{\sqrt{q^2 + r^2 + z^2} - 2rq}{(q^2 + r^2 + z^2)^2 - (2rq)^2} \times E_2 \left[-\frac{4rq}{(q-r)^2 + z^2} \right], \quad (16)$$

where I is the isotropic, frequency-integrated intensity, and E_2 is the complete elliptical integral of the second kind (Abramowitz & Stegun 1965, p. 590). For the temperature stratifications of interest, this expression for dJ cannot be integrated analytically over q to give J . Resorting to a one-dimensional numerical integration, Figure 4 shows J and F as function of X for the SHS disk at a representative r_0 . Importantly, for the outer wind, the critical point lies upstream of the maximum of both J and F . Since J increases along the streamline while the electron density drops, ξ increases all the way to the critical point, as in O-star winds. The line force at the critical point is, therefore,

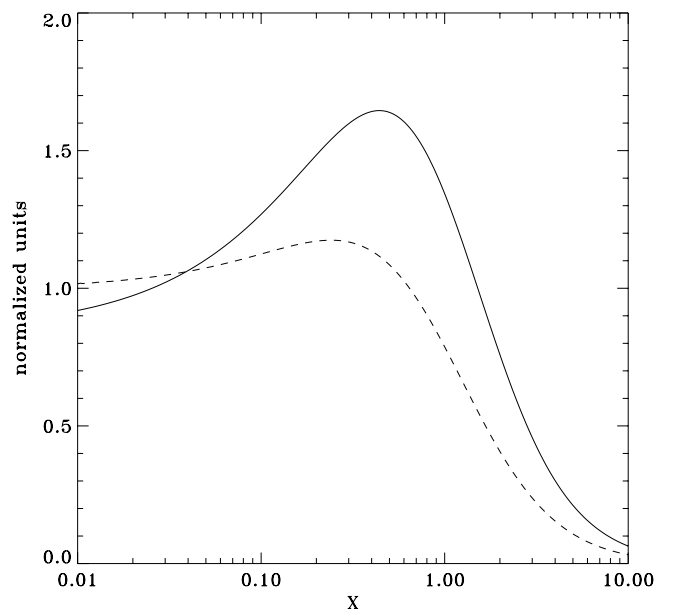


FIG. 4.—Normalized, projected flux (solid line) and mean intensity (dashed line) above the SHS disk ($r_d = 30r_{wd}$) along a ray with footpoint $r_0 = 10r_{wd}$ and $\lambda_{cr} = 58^\circ$.

smaller for $\delta > 0$ than for $\delta = 0$, and the same is true for the mass-loss rate. Alternatively, in the unlikely situation that the wind recombines along the streamline, the driving force as well as the mass loss would increase because of a larger number of metal transitions.

To understand the effect of ionization stratification on the wind velocity law, we include the δ -correction above the critical point but neglect it below the same, thereby leaving the mass-loss rate unaltered. Since the δ -term introduces a dependence of the line force on W besides that on W' , the solution to the Euler equation has to be iterated until convergence is achieved.

We find that, assuming $\alpha = \frac{2}{3}$ and $\delta = 0.2$, terminal speeds decrease by a factor of ~ 2 for outer regions of the SHS disk, whereas the optical depth t increases by a factor of ~ 4 , thereby pushing the solution further away from the cutoff at $t \sim 10^{-7}$. For inner disk regions, the effect of δ on v_∞ and t is less pronounced. The somewhat ambivalent conclusion is, therefore, that δ -terms may, as desired, raise t by a factor of a few but, at the same time, also lead to an unwanted reduction in terminal speeds.

6. DISCUSSION

In this section, we compare the mass-loss rates from our model with values quoted in the literature, which are typically estimated from P Cygni line fits or from dynamical wind modeling. We also mention briefly some processes neglected in this work that may have an effect on \dot{M} .

6.1. Comparison with \dot{M} from Kinematical Wind Modeling

The most reliable estimates for mass-loss rates from CVs are, so far, from P Cygni line fits. For nova-like variables with parameters similar to those considered here, Vitello & Shlosman (1993) and Knigge et al. (1995) find a lower limit of $\sim 10^{-2}$ to the ratio of mass-loss to accretion rates. Below this value, the observed line profiles cannot be reproduced because the wind becomes overionized. This is about 2 orders of magnitude larger than \dot{M} derived in § 4, when $Q = 2000$ is used as in O stars. It is important, however, that a highly idealized blackbody disk spectrum was used in the line fitting. This is a clear overestimate of the ionizing radiation in the Lyman continuum (Polidan et al. 1990; Long et al. 1991, 1994; van Teeseling et al. 1993; Knigge et al. 1997). For a more realistic radiation field that accounts for the Lyman cutoff, the wind mass-loss rate can be reduced while maintaining the same ionization parameter.

As is shown in Figure 5, we have been able to reproduce acceptable P Cygni line profiles down to $\dot{M} \sim 10^{-11} M_\odot \text{ yr}^{-1}$ for a generic wind model. We use the Lyman cutoff and a tail of high-energy X-rays to account for carbon ionization. Essentially, all the carbon is then in the form of C IV because of Auger ionization of C II by X-rays. For $\dot{M} \sim 10^{-12} M_\odot \text{ yr}^{-1}$, on the other hand, the emission component in the calculated line profile is missing, which is in disagreement with observations (Fig. 5).

6.2. Comparison with \dot{M} from Dynamical Wind Modeling

Next, we compare the mass-loss rates from our analytical wind model with those from dynamical simulations of disk winds. The only realistic dynamical modeling of CV disk winds attempted so far was performed by PSD. We have provided a general comparison between our model and theirs in Paper I and turn here to mass-loss rates.

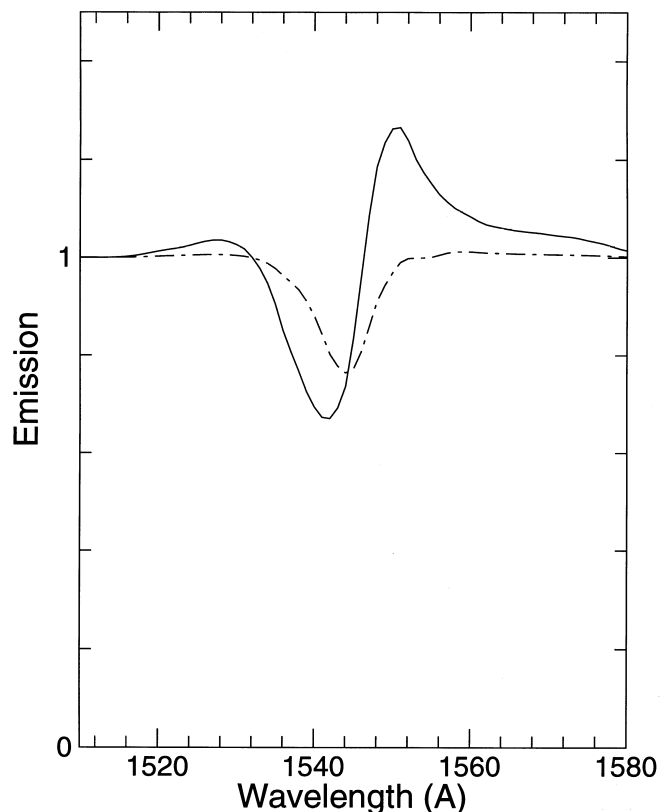


FIG. 5.—Synthetic P Cygni line profiles for an LDW from a disk with suppressed Lyman continuum. The wind mass-loss rate is $\sim 10^{-11} M_\odot \text{ yr}^{-1}$ (solid line) and $\sim 10^{-12} M_\odot \text{ yr}^{-1}$ (dashed line).

Using $k = 0.2$ and $\alpha = 0.6$, PSD find for the SHS disk mass-loss rates of $\dot{M} = 5 \times 10^{-14} M_\odot \text{ yr}^{-1}$ and $\dot{M} = 5 \times 10^{-12} M_\odot \text{ yr}^{-1}$, corresponding to disk luminosities of $L_d = 8 L_\odot$ and $L_d = 24 L_\odot$, respectively. It is clear that such an increase by a factor of 100 in \dot{M} cannot be understood from the simple CAK scaling, $\dot{M} \propto L^{1/\alpha}$. Instead, this strong dependence on L_d is a consequence of the optically thick-to-thin transition in the disk LDW when $Q \Gamma \sim 1$, as is also discussed by Proga (1999). Since PSD apply an exponential line-list cutoff (Owocki et al. 1988), the force multiplier $M(t)$ reaches a maximum in optically thin flow regions. This suppresses the mass-loss rate as compared with the case of a pure power-law force multiplier.

Even for a low-luminosity disk, PSD find that large \dot{M} can be driven, namely when α is as large as 0.8. However, PSD assume the same value of $k = 0.2$ for all α . As is evident from Figure 4 of Gayley (1995), k drops by a factor of 10 when α is increased from 0.6 to 0.8, leading to a very similar \dot{M} in both cases. This is a consequence of $Q \Gamma \sim 1$ for a disk wind (see eq. [12]). Contrary to this, for O-star winds, $Q \Gamma \gg 1$; hence, \dot{M} depends strongly on α .

For a more luminous disk with $L_d = 24 L_\odot$, we estimate $\dot{M} \simeq 4 \times 10^{-12} M_\odot \text{ yr}^{-1}$ from equation (12) when a value of D is used characteristic of the narrow wind base of PSD. The agreement with $\dot{M} = 5 \times 10^{-12} M_\odot \text{ yr}^{-1}$ as found by PSD is very good.

6.3. The Mass-Loss Paradigm in Disk Winds from CVs

Analysis of LDWs from O stars revealed $Q \Gamma$ to be the key parameter determining the mass-loss rate in the wind

(Gayley 1995). Namely, for $Q\Gamma < 1$, the wind ceases to exist. For O stars, $Q\Gamma > 100$, producing a kind of a “safety belt.” The situation is different for winds from luminous CV disks, where $Q\Gamma \sim 1$, if the O-star value for Q is used (this work and PSD).

Taken at face value, the modified CAK theory of LDWs from CV disks predicts therefore surprisingly low mass-loss rates if $Q = 2000$. The calculated rates of $\dot{M} \sim 10^{-12} M_{\odot} \text{ yr}^{-1}$ for $L_d = 10 L_{\odot}$, or even lower, when the saturation of the force multiplier is accounted for, imply that LDWs will have a thick-to-thin transition in the strongest driving lines and will have difficulties in reproducing the observed line profiles. What are the possible solutions to this problem?

First, higher values of Q are the most obvious way to increase \dot{M} in the wind. The value of Q is rather uncertain. It is especially unclear how the different spectral shape of the disk radiation field and its effect on the non-LTE occupation numbers will modify Q as compared with its O-star value. Such calculations have never been attempted and are clearly beyond the scope of this paper. Theoretically, the value of Q can be significantly larger than that for the O stars.

Second, a situation could arise in disk winds where the wind is driven by photons from a part of the disk that is UV bright, while the ionization is controlled by the central disk region, e.g., the boundary layer, which is X-ray bright. This, again, will be especially pronounced in the presence of a Lyman-continuum cutoff in the UV source. Under these circumstances, given the wind overionization, the line force will be reduced below its CAK value (MacGregor, Hartmann, & Raymond 1979; Fransson & Fabian 1980) and, hence, the velocity gradient will be small as well. A shallow velocity law will increase the overall optical depth in the wind and push the thick-to-thin transition downstream, away from the critical point. It is important in this context that the observed small changes in the P Cygni line profiles in eclipsing nova-like CVs *require* very shallow velocity profiles in the wind (Shlosman, Vitello, & Mauche 1996).

Additional factors can affect the mass-loss rates to a lesser degree. (1) Allowing for streamlines to bend will result in a better alignment with the radiative flux vector, which should increase the mass loss. (2) Pauldrach & Puls (1990) find a sudden increase in stellar mass-loss rates of B supergiants when the Lyman continuum becomes optically thick at the wind base, e.g., when the effective temperature drops below a certain threshold or if Γ reaches some critical value. This induces a shift to lower wind ionization, which, in turn, increases the mass loss (more driving lines), increases the Lyman jump even more, and so on, until a stable situation with high \dot{M} and low wind ionization is reached. (3) Furthermore, Q depends linearly on the wind metallicity, and enhanced metal abundances could lead to a larger $Q\Gamma$,

which governs the mass loss. This is particularly significant to the He abundance because of the efficient convection in the low-mass secondary stars but may be relevant to metals as well.

7. SUMMARY

The focus of this second paper on line-driven winds from accretion disks in cataclysmic variables is on theoretical estimates of mass-loss rates and wind velocity laws. Our results are as follows.

The mass-loss rates derived from applying the modified CAK formalism appear to be substantially smaller than those inferred from P Cygni line fits, even with a suppressed Lyman continuum, and are more so when the saturation effect in the line-force multiplier is included. Yet these rates are in good agreement with results from time-dependent, two-dimensional dynamical wind simulations by PSD. The reason for low mass-loss rates is that the key parameter controlling LDWs, $Q\Gamma \sim 100$ for O-star winds, is only ~ 1 for disk winds when O-star values for Q are used. Some potential resolutions to this problem were proposed.

We find that the mass loss is dominated by the inner decade in disk radii. For Shakura & Sunyaev and Newtonian disks, the mass loss per unit radius is roughly uniform out to five white dwarf radii and drops $\propto r_0^{-1.9}$ and $r_0^{-0.8}$ at larger r_0 , respectively. Because of their low mass-loss rates, CV disk winds should experience a thick-to-thin transition even in the strongest driving lines. These winds should, therefore, resemble more closely winds of B stars near the main sequence than that of O supergiants.

The wind velocity profiles show a slowly accelerating flow, with a characteristic acceleration length given by the footpoint radius of the streamline in the disk. Fitting the observed line profiles using kinematical models suggests even slower accelerating winds. The observable terminal velocity of the wind is associated with the thick-to-thin transition in the driving lines. Given this latter fact, and given uncertainties in the ionization stratification and in the anticipated streamline bending at large radii, the actual wind terminal velocity is poorly constrained in our model.

We are grateful to Jon Bjorkman, Rolf Kudritzki, Chris Mauche, Norman Murray, Stan Owocki, and Joachim Puls for numerous discussions on various aspects of line-driven winds. I. S. acknowledges hospitality of the IGPP/LLNL, where this work was initiated, and of its director, Charles Alcock. This work was supported in part by NASA grants NAG 5-3841 and WKU-522762-98-06, and HST G0-06546.02-95A and AR-07982.01-96A (I. S.), and was performed under the auspices of the US Department of Energy by LLNL user contract number W-7405-ENG-48 (P. V.).

APPENDIX

DISK EDDINGTON FACTORS REQUIRED FOR LINE-DRIVEN WINDS

Using the eigenvalues E_{cr} from Paper I, one can further quantify the disk Eddington factors required to launch a line-driven wind that is optically thick at least up to the critical point. Consider first a vertical wind above an infinite, isothermal disk. The Euler equation (5) becomes, for $\tilde{F}_x = 1$ (the flux component along \hat{x} , normalized to the footpoint flux),

$$W' = -g + \Gamma(r_0)M(t_x). \quad (\text{A1})$$

From equation (18) in Paper I, at the critical point,

$$\Gamma(r_0) = \frac{2/3\sqrt{3}}{(1-\alpha)M_{\text{cr}}(t)}. \quad (\text{A2})$$

Since the maximum of $M(t)$ for a gas of solar composition is ~ 2000 (Abbott 1982), one has that $\Gamma(r_0) \gtrsim 4 \times 10^{-4}$ for all r_0 . Next, for the more realistic case of a tilted wind above a disk with radial temperature stratification, the simplified Euler equation (5) reads

$$W' = -g + \Gamma(r_0) \tilde{F}_x M(t_x). \quad (\text{A3})$$

Using $W'_{\text{cr}} = (\alpha/1-\alpha)g_{\text{cr}}$ and assuming $g_{\text{cr}} \simeq X_{\text{cr}}$ for critical points close to the disk,

$$\Gamma(r_0) = \frac{X_c}{(1-\alpha)\tilde{F}_x(r_0, X_{\text{cr}})M_{\text{cr}}(t)}. \quad (\text{A4})$$

According to Figure 5 in Paper I, $\tilde{F} < 4$; hence, $\Gamma(r_0) \gtrsim 10^{-4}$ is required for the wind to be optically thick at the critical point.

REFERENCES

- Abbott, D. C. 1982, *ApJ*, 259, 282
 Abramowitz, M., & Stegun, I. A., ed. 1965, *Handbook of Mathematical Functions* (New York: Dover)
 Cassinelli, J. P. 1994, *Ap&SS*, 221, 277
 Cassinelli, J. P., Cohen, D. H., MacFarlane, J. J., Sanders, W. T., & Welsh, B. Y. 1994, *ApJ*, 421, 705
 Castor, J. I., Abbott, D. C., & Klein, R. I. 1975, *ApJ*, 195, 157 (CAK)
 Feldmeier, A., & Shlosman, I. 1999, *ApJ*, 526, 344 (Paper I)
 Fransson, C., & Fabian, A. C. 1980, *A&A*, 87, 102
 Gayley, K. G. 1995, *ApJ*, 454, 410
 Hoare, M. G., & Drew, J. E. 1993, *MNRAS*, 260, 647
 Knigge, C., Long, K. S., Blair, W. P., & Wade, R. A. 1997, *ApJ*, 476, 291
 Knigge, C., Woods, J. A., & Drew, J. E. 1995, *MNRAS*, 273, 225
 Kudritzki, R. P., Springmann, U., Puls, J., Pauldrach, A., & Lennon, M. 1998, in *ASP Conf. Ser. 131, Boulder-Munich II: Properties of Hot, Luminous Stars*, ed. I. Howarth (San Francisco: ASP), 278
 Long, K. S., et al. 1991, *ApJ*, 381, L25
 Long, K. S., Wade, R. A., Blair, W. P., Davidsen, A. F., & Hubeny, I. 1994, *ApJ*, 426, 704
 MacGregor, K. B., Hartmann, L., & Raymond, J. C. 1979, *ApJ*, 231, 514
 Mauche, C. W., & Raymond, J. C. 1987, *ApJ*, 323, 690
 Murray, N., & Chiang, J. 1996, *Nature*, 382, 789
 Owocki, S. P., Castor, J. I., & Rybicki, G. B. 1988, *ApJ*, 335, 914
 Pauldrach, A., & Puls, J. 1990, *A&A*, 237, 409
 Pauldrach, A., Kudritzki, R. P., Puls, J., Butler, K., & Hunsinger, J. 1994, *A&A*, 283, 525
 Polidan, R. S., Mauche, C. W., & Wade, R. A. 1990, *ApJ*, 356, 211
 Prinja, R. K., & Rosen, S. R. 1995, *MNRAS*, 273, 461
 Proga, D. 1999, *MNRAS*, 304, 938
 Proga, D., Stone, J. M., & Drew, J. E. 1998, *MNRAS*, 295, 595 (PSD)
 Puls, J. 1987, *A&A*, 184, 227
 Puls, J., Springmann, U., & Lennon, M. 1999, in preparation
 Puls, J., Springmann, U., & Owocki, S. P. 1998, in *Cyclical Variability in Stellar Winds*, ed. L. Kaper & A. W. Fullerton (Berlin: Springer), 389
 Shakura, N. I., & Sunyaev, R. A. 1973, *A&A*, 24, 337 (SHS)
 Shlosman, I., & Vitello, P. 1993, *ApJ*, 409, 372
 Shlosman, I., Vitello, P., & Mauche, C. W. 1996, *ApJ*, 461, 377
 van Teeseling, A., Verbunt, F., & Heise, J. 1993, *A&A*, 270, 159
 Vitello, P., & Shlosman, I. 1988, *ApJ*, 327, 680
 ———. 1993, *ApJ*, 410, 815